

Determination of Directivity of Microwave Antennas using IR Thermography

Khalid Muzaffar

Assistant professor, Department of Electronics & Communication Engineering,

Islamic University of Science & Technology, Awantipora

Abstract—The Directivity of microwave antennas can easily be determined using infrared thermography. An absorption screen made up of some carbon loaded polymer is placed in front of an antenna. The electromagnetic waves impinging the screen are partially absorbed by it, resulting in its temperature rise. This temperature rise is monitored by an infrared camera. These thermal images captured by the thermal camera on processing give the electric power distribution at the screen location. The half power points on the radiation pattern of an antenna can be easily located from which half power beam widths in both E and H planes can be calculated. From these beam widths, directivity is then calculated.

The experiments were carried with a patch antenna radiating at 8 GHz. In order to show the repeatability, experiments were carried for different distances between patch antenna and absorption screen. A great agreement was seen between experimental (thermographic results) and measurement results.

The microwave source is modulated at a low frequency so as to permit Lock-in thermography to detect even small temperature changes on the screen.

Index Terms—Ceramics, thermograph, coaxial resonators, delay filters, delay-lines, power amplifiers.

I. INTRODUCTION

Infrared thermography has been widely for characterization of electromagnetic fields [1]-[11]. Fig.1 shows the mock-up of thermographic measurement setup. A thin screen of a carbon loaded polymer is placed in front of an antenna. This screen is minimally perturbing unlike the metallic probes. The electromagnetic waves falling on the screen produce heating effects as per joules law. This temperature rise is monitored by an infrared camera. The temperature rise (ΔT) on the screen is related to electric field magnitude (E) at the screen surface by (1) as reported in [8].

$$E = k\sqrt{\Delta T} \quad (1)$$

Where k is a constant.

II. MEASUREMENT PRINCIPLE

The principle of this measurement technique can be understood from Fig.2. The patch antenna radiating at 8 GHz is connected to a synthesized signal generator which is turned

ON/OFF at a frequency of 1Hz. The temperature variation on the screen is monitored by an IR camera. The infrared camera is taking thermal images of the screen at

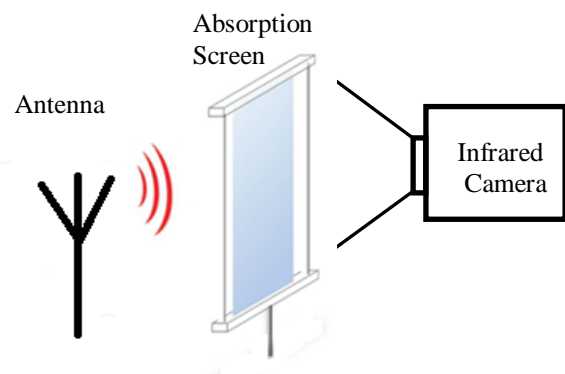


Fig. 1. Thermographic measurement setup.

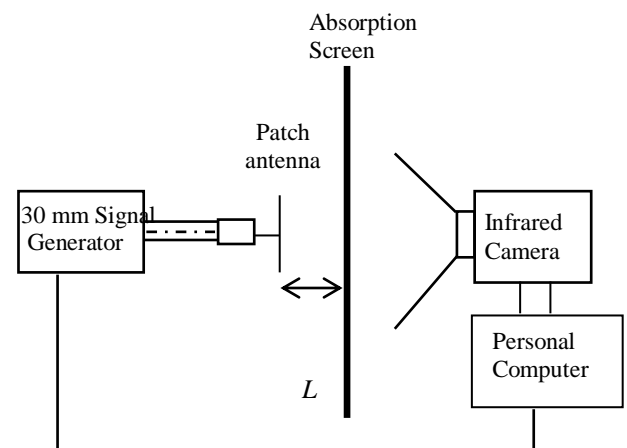


Fig. 2. Block diagram of experimental set-up.

20Hz. The data captured by the camera is stored in a computer attached to it. Fourier transformation of the recorded thermal movie at 1Hz gives an amplitude image corresponding to the temperature change on the screen which is proportional to square of electric field magnitude as per (1). From this amplitude image we determine the half power points in both E and H planes and hence calculate half power beam widths for E and H planes. The half power points on the thermograph are the points with temperature half of the maximum temperature

(T_{max}). Further from these beam widths the directivity can then be calculated. The infrared camera used is 14-bit, 320x420 resolution, medium wave IR (MWIR) from FLIR.

III. ANTENNA DESCRIPTION

Fig. 3 shows an 8 GHz patch antenna used in the experiments Fig. 4 shows the schematic diagram of the patch antenna. The thickness of the dielectric material used for the patch antenna is 0.762 mm and its relative permittivity ϵ_r is 2.2. The size of radiating patch is 14.7 mm x 12.3 mm. The various dimensions of the antenna are shown in the Fig. 4.

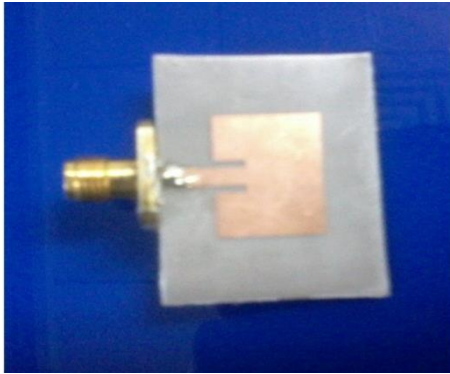


Fig. 3. 8 GHz patch antenna.

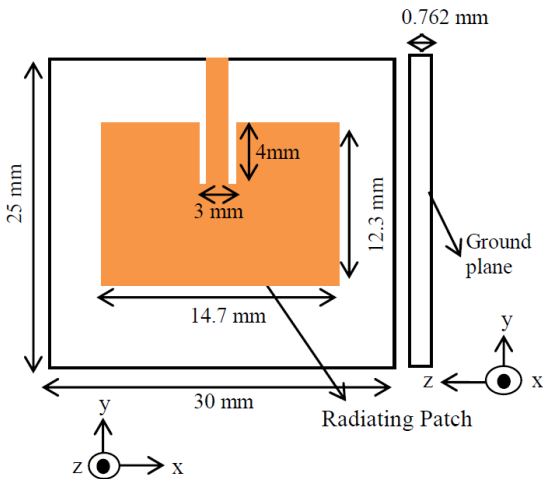


Fig. 4. Geometrical details of the 8 GHz antenna.

IV. RESULTS AND CALCULATIONS

The absorption is kept at different distances ($L=60mm, 70mm, 80mm$) from the patch antenna. The thermographs corresponding to these distances are shown in Figs 6-8. Two points each on two central lines $x=0$ or $y=0$ on the thermograph, where the temperature is half of the maximum temperature, correspond to half power points in E-plane and H-plane respectively. The distance d between these

points is obtained from the thermograph and beam width (BW) is then calculated using (2) as obtained from Fig.5.

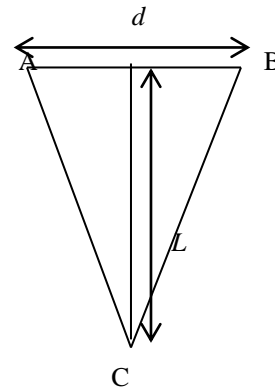


Fig. 5. Geometric diagram for Beam width calculation.

$$BW = 2 \tan^{-1}(d / 2L) \tag{2}$$

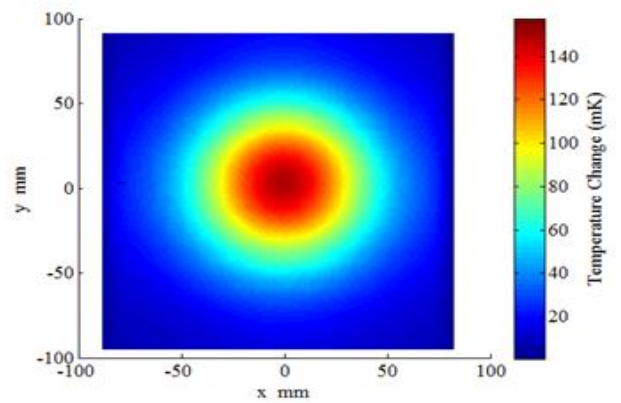


Fig.6. Thermograph showing temperature distribution on absorption screen for $L=60mm$.

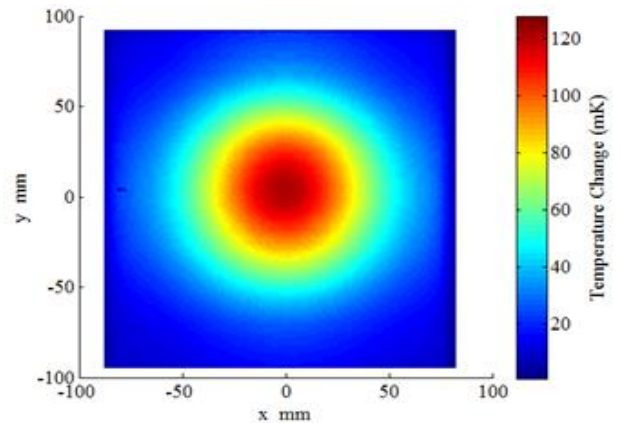


Fig.7. Thermograph showing temperature distribution on absorption screen for $L=70mm$

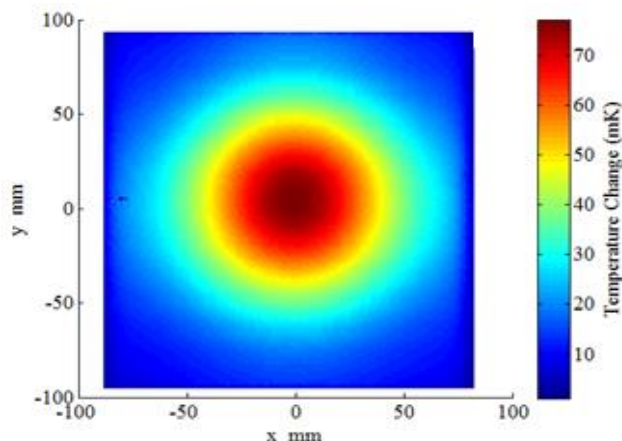


Fig.8. Thermograph showing temperature distribution on absorption screen for $L= 80\text{mm}$.

The Directivity (D) is calculated using equation (3)

$$D = \frac{4\pi}{(\theta_E)(\theta_H)} \left(\frac{180}{\pi}\right)^2 = \frac{41253}{(\theta_E)(\theta_H)} \quad (3)$$

Distance (L) of the absorption screen from patch antenna (in mm)	Distance (dE) between half power points in E – plane(in mm)	Distance (dH) between half power points in H – plane(in mm)	Beam width E – plane θ_E (in degrees)	Beam width H – plane θ_H (in degrees)	Directivity (D)
60	93.23	93.417	75.69	75.80	7.19
70	108.38	108.55	75.49	75.58	7.23
80	123.17	123.37	75.18	75.27	7.29

References

[1] R. M. Sega; J. D. Norgard, "Infrared Measurements of Scattering and Electromagnetic Penetration through Apertures," *IEEE Transactions on Nuclear Science*, vol.33, no.6, pp.1657-1663, Dec. 1986.

[2] J. D. Norgard, "Electromagnetic magnitude and phase measurements from infrared thermograms," *Aerospace Conference, 1997. Proceedings, IEEE*, vol.2, pp.145-157 vol.2, 1-8 Feb 1997.

[3] J. D. Norgard; J. Will; C. F. Stubenrauch, "Quantitative images of antenna patterns using infrared thermography and microwave holography," *Int. J. Imag. Syst. Tech.*, vol. 11, n. 4, special issue on "Advances in quantitative image analysis," pp. 210-218, Jul.-Aug. 2000.

[4] J. Norgard and Musselman, "CEM code validation using infrared thermograms," *International symposium on electromagnetic compatibility*, pp. 637-640 (2004).

[5] J. E. Will, J. D. Norgard , R. M. Sega , M. Seifert , A. Pesta and J. Cleary "Determining Antenna Near Field Magnitude Data Using Infrared Thermographic Measurements," *Proceedings of the 18th Annual Symposium of the Antenna Measurement Techniques Association*, pp.193 -197 1996.

[6] J. Will, J. Norgard, C. Stubenrauch, K. MacReynolds, M. Seifert and R. Sega "Phase Measurements of Electromagnetic Fields Using Infrared Imaging Techniques and Microwave Holography," *Proceedings of the SPIE Aerosense Conference, Conference*, vol. 2766, 1996.

- [7] N. Chiyo, M. Arai, Y. Tanaka, A. Nishikata, T. Hirano, T. Maeno, "Measurement technique for electromagnetic field intensity distribution using infrared 2-D lock-in amplifier," *2010 Annual Report Conference on Electrical Insulation and dielectric*.
- [8] K. Muzaffar , S. Tuli, and S. Koul, "Infrared Thermography for Electromagnetic Field Pattern Recognition," *International Microwave and RF Conference, IMARC-2013*, pp. 1-4, 14-16 Dec. 2013.
- [9] K. Muzaffar, S. Tuli and S. Koul "Beam width estimation of microwave antennas using infrared thermography", *Infrared Physics & Technology* 72(Sep. 2015), 244-248.
- [10] Khalid Muzaffar, Suneet Tuli and Shibam Koul "Determination of Polarization of Microwave signals by Lock-in Infrared Thermography", *IETE Journal of Research* (Oct. 2015).
- [11] K. Muzaffar, L.I. Giri, K. Chatterjee, S. Tuli, S. Koul, "Fault detection of antenna arrays using infrared thermography", *Infrared Phys. Technology* 71 (July 2015), 464-468.